# Suction-induced effects on the seismic response of a zoned earth dam through simplified dynamic analyses

*Lucia* Coppola[1*], *Mariagrazia* Tretola[2], *Stefania* Sica[2], *Luca* Pagano[1]

[1]University of Naples Federico II, Department of Civil, Architectural and Environmental Engineering, Naples, Italy

[2]University of Sannio, Department of Engineering, Benevento, Italy

**Abstract.** In zoned earth dams, the contrast in hydraulic conductivity between the core and the shells causes the saturation line to drop across the core, leaving most of the downstream shell in an unsaturated state. Since suction provides for additional stiffness and strength to soil, the paper investigates the contribution of suction-induced effects in the downstream shell and other dam zones located above the saturation line on the seismic response of the dam. To this aim, a Newmark-based approach has been adopted. The seismic response of the dam is first analysed by equivalent linear dynamic analyses to obtain the equivalent acceleration acting throughout the sliding mass, which is then employed in the application of the Newmark method. Since critical surfaces for zoned earth dams are those crossing the core, the study focuses on sliding mechanisms involving these surfaces.

## 1 Introduction

In recent years, considerable attention has been devoted to earthquake-induced instability phenomena affecting large earth dams, many of which were constructed without specific seismic design regulations.

Previous studies [1] indicate that the most frequently reported issues in case histories of dams damaged by strong earthquakes—documented in ICOLD Bulletins [2] and various scientific publications [3, 4, 5]- typically concern phenomena such as freeboard loss, slope instability, cracking or erosion of watertight elements, and soil liquefaction [6, 7, 8, 9]. Earth dams may undergo slope sliding during strong earthquakes, potentially involving small to large portions of the dam body. When the dam watertight element is also affected by sliding, particular attention must be paid to assessing the dam safety with respect to deformation phenomena that could compromise its hydraulic retention capacity [10].

In the case of zoned earth dams, among the various damage mechanisms that may be triggered by an earthquake, particular attention should be given to evaluating the magnitude of sliding along surfaces that cross the core, as such displacements could severely compromise the dam watertightness. For this specific purpose, Newmark-based methods represent suitable predictive tools.

Among the simplified methods, a central role is played by the sliding-block method developed by Newmark (1965) [11] and later refined by other researchers [12, 13]. The derived approaches use an "equivalent acceleration" obtained from an initial seismic analysis of the dam, where the soil is considered deformable. The equivalent acceleration, driving the rigid Newmark block, incorporates the dam geometry as well as the stiffness and damping characteristics of the soil [14].

In zoned earth dams, the contrast in hydraulic conductivity between the core and the shells determines the saturation line to drop throughout the core, leaving most of the downstream shell in an unsaturated state. To the best of the authors' knowledge, only a few publications in the literature address the issue of partial saturation regimes that may occur above the saturation line when studying the seismic response of dams [15, 16, 17] and their impact in terms of seismic-induced settlements.

As suction provides additional stiffness and strength to soil, the present paper analyses the consequences of considering or not suction in the downstream shell and other dam zones above the saturation line.
Using the Conza dam in Italy as a reference case, the paper compares the predicted permanent settlements under full impounding conditions, both considering and ignoring the effects of the unsaturated zones.

* Corresponding author: lucia.coppola@unina.it

# 2 The case study

## 2.1. The Conza dam

The Conza Dam is situated on the Ofanto River, between the Campania and Puglia regions (Figure 1), in southern Italy.

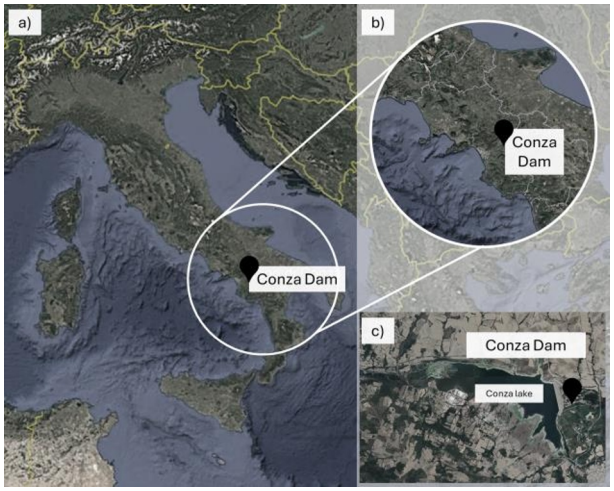


**Fig. 1.** Google earth view of the localization of the Conza dam within a) national, b) regional framework; c) view of Conza dam and Conza Lake.

This zoned earth dam has an internal clay core (Figure 2). The construction of the dam took place from 1979 to 1988, aiming to create a reservoir with a capacity of 77.4 million cubic meters. The foundation consists of an over-consolidated clay layer extending in depth to several hundred meters, with some areas covered by alluvial deposits. The dam reaches a maximum height of approximately 47 meters, measured from the deepest level of the core foundation, which rests directly on the clay layer. The core consists of medium plasticity clay; the shells are made of coarse-grained materials derived from the alluvial deposits. The core filters were obtained from removing the coarser gravel components from the alluvial material.

The dam spans 880 meters longitudinally, with a cross-section that remains quite invariable, except for variations in the thickness of the alluvial layer.

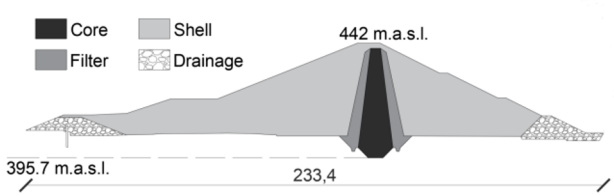


**Fig. 2.** The Conza dam

## 2.2. Materials

Three pairs of new boreholes, drilled in 2019, allowed for a detailed the characterisation of material properties for core, filters, shells, and foundation.

Two of them started from the crest and intercepted the core and the filters; the third started from the first downstream bank and traversed the downstream shell.

### *2.2.1 Core*

The clay core consists of sandy silt with clay.
Based on Consolidated Isotropically Drained (CID) and Undrained (CIU) triaxial tests conducted on undisturbed samples, the following mean values were derived:
• effective friction angle ($\phi$') = 22.6°
• effective cohesion (c') = 45.5 kPa
• undrained cohesion ($c_u$) = 146.9 kPa.
The hydraulic conductivity coefficient was estimated based on the oedometric test and resulted in $2.9*10^{-11}$ $ms^{-1}$.

### *2.2.2 Filters*

The material constituting the filters had a homogeneous composition, ranging from silt with sand and clay to gravelly-silty sand.

Undisturbed samples were tested through Consolidated Isotropically Drained (CID) tests, and the following mean strength parameters were obtained:
• effective friction angle ($\phi$') = 23.1°
• effective cohesion (c') = 43.5 kPa

The hydraulic conductivity coefficient, estimated from variable head permeability tests, averaged $6.4*10^{-6}$ $ms^{-1}$.

### *2.2.3 Shells*

The material constituting the shells consists of sand with gravel.

Direct shear tests conducted on large samples yielded the following mean strength parameters:
• effective friction angle ($\phi$') = 44°
• effective cohesion (c') = 8.8 kPa

The hydraulic conductivity coefficient, estimated from variable head permeability tests, averaged $4.7*10^{-6}$ $ms^{-1}$.

# 3 Methodology

Table 1 summarizes the four different approaches followed to characterise the dam seismic response in terms of sliding displacement magnitude, accounting or not for the effects of the soil unsaturated state above the saturation line. The shear modulus (G) is a function of vertical effective stress ($\sigma'_v$) and the shear strength is computed according to the equation (1) proposed by Fredlund et al. (1979) [18]

$$\tau_{lim}=c'+\sigma_n \tan\phi'+(u_a-u_w)\tan\phi_b \quad (1)$$

where:
• $u_a$ is the pore-air pressure;
• $u_w$ is the pore-water pressure;

• $\phi_b$ is the angle regulating the increase in strength due to suction.

In the present work, $\phi_b$ is taken to be about $\phi'/3$, as suggested in common practice.

In the following, accounting for suction-induced stiffness corresponds to considering $\sigma'_v$ increased by suction, while suction-induced strength to quantifying the last term of Eq.1.

Approach #1 considers the downstream shell completely dry without any account for the suction effect.

Approach #2 considers the effect of suction on the stiffness of the portion of dam characterized by non-null suction, neglecting it on soil strength.

Approach #3 considers the effect of suction on the strength of the portion of dam characterized by non-null suction.

Approach #4 considers both effects generated by suction on soil stiffness and strength.

**Table 1** Methodology.

| Approach | Without suction effect | With suction effect on soil | |
|---|---|---|---|
| | | Stiffness | Strength |
| #1 | x | | |
| #2 | | x | |
| #3 | | | x |
| #4 | | x | x |

For each approach, the distribution of pore water pressure is obtained through a two-dimensional seepage analysis, based on the solution of Richard's equation [19], through the FEM code Geostudio [20].

The distribution of pore water pressure (positive or negative) is obtained considering the conditions of full impounding. On the dam crest, downstream shell and downstream ground surface, a seepage surface condition is applied, as suggested by Heitland et al., (2020) [21].

Subsequently, equivalent linear dynamic analyses [20] were carried out by implementing the effective stress changes generated by the computed pore water pressures and the signals provided by seismological studies. The accelerometric records were selected from the PEER (Pacific Earthquake Engineering Research Center) Ground Motion Database.

The outcomes of the equivalent linear dynamic analyses were subsequently used to apply the Newmark method [11] for the computation of the permanent displacements. The accelerogram signal processed by the Newmark method is the equivalent acceleration acting throughout the unstable mass.

The four different approaches proposed above are compared in terms of peak ground acceleration profiles along the core and maximum settlement along the sliding surface.

## 4 Results and discussion

Figure 2 shows the results of the seepage analysis.

It can be noted that the saturation line drops abruptly within the core, determining the downstream shell suction values ranging between 0 kPa and about +200 kPa.

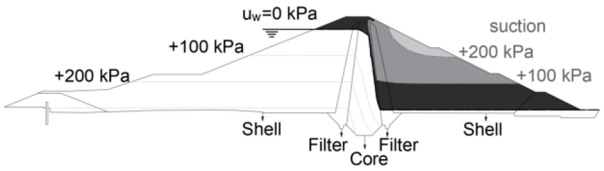


**Fig. 2.** Distribution of pore water pressure and suction within the dam.

Figure 3 compares the profiles of peak ground acceleration (PGA) in the x- and y-direction for the four approaches (Table 1) along section 1 crossing the core.

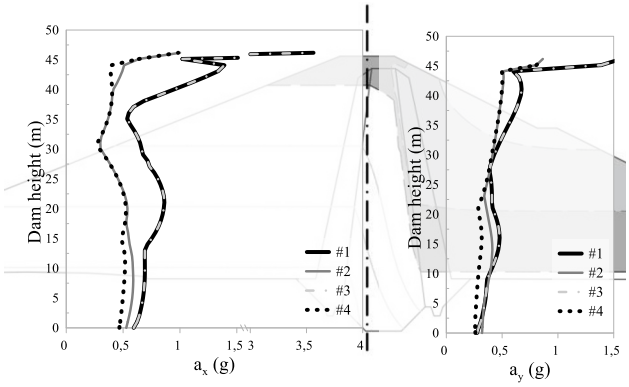


**Fig. 3.** Horizontal ($a_x$) and vertical ($a_y$) peak ground acceleration profiles along the core axis.

Approaches #1 and #3, which neglect the effects of suction-induced stiffness, and #2 and #4, which consider it, yield results that overlap by two to two being processed with the same stiffness. The former two show, as expected, higher amplification with elevation based on lower stiffness levels. The differences occur at any elevation due to downstream shell suction acting throughout it.

The PGA profiles in the vertical direction ($a_y$) result strongly consistent with those investigated in x-direction. Figure 4 shows the slip surface considered for the comparison of the computed permanent displacements.

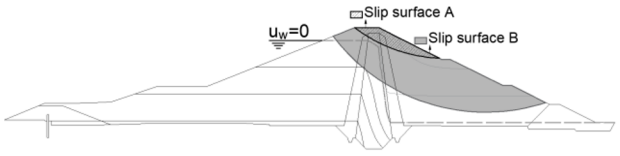


**Fig. 4.** Slip surface considered for pseudo-dynamic analyses.

Slip surface A starts from the crest and is almost completely included within the partially saturated zone. Slip surface B crosses the core, embraces the crest, and passes through the downstream shell.

Table 2 reports the settlements computed for surfaces A and B according to the four approaches. The same table also reports the maximum settlement computed by each approach, relating to the different surfaces plotted in Figure 5.

For the most significant surface crossing the core (B), approach #1 displacements are at the highest due to higher amplification and less strength. Increasing the shear stiffness due to suction without altering strength (approach #2) implies a significant reduction in permanent displacements. Considering suction strength (approaches #3 and #4) implies permanent displacement nullification.

**Table 2** Results of Newmark analyses.

| Sliding surface | Settlement (cm) | | | |
|---|---|---|---|---|
| | Approach #1 | Approach #2 | Approach #3 | Approach #4 |
| A | 10 | 0 | 0 | 0 |
| B | 1.2 | 0.8 | 0 | 0 |
| max | 31 | 17 | 12 | 2 |

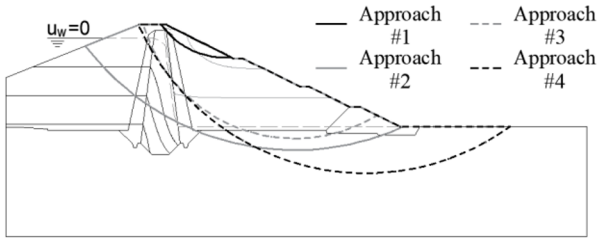


**Fig. 5.** Sliding surface corresponding to the maximum settlement from the Newmark analysis.

## 5 Conclusions

The paper highlights that suction acting above the saturation line of a zoned earth dam can lead to results significantly different from those predicted by traditional approaches that neglect it. Accounting for suction-induced stiffness increases implies non-negligible differences, while including the additional contribution of suction-induced strength may be crucial in assessing the dam performance to seismic loads.

This study was carried out within the RETURN Extended Partnership and received funding from the European Union Next-GenerationEU (National Recovery and Resilience Plan – NRRP, Mission 4, Component 2, Investment 1.3 – D.D. 1243 2/8/2022, PE0000005).

## References

[1]. Costigliola, R. M., Mancuso, C., Pagano, L., & Silvestri, F. (2022). Prediction of permanent settlements of an upstream faced earth dam. *Computers and Geotechnics*, *144*, 104594. (2022) https://doi.org/10.1016/j.compgeo.2021.104594

[2]. Icold, 2001. Design features of dams to effectively resist seismic ground motion. International Commission On Large Dams, Paris, Bulletin, p. 120. (2001)

[3]. Sica, S., & Pagano, L.. Performance-based analysis of earth dams: procedures and application to a sample case. Soils and foundations, 49(6), 921-939. (2009) https://doi.org/10.3208/sandf.49.921

[4]. Wieland, M.. Seismic aspects of dams. *General Report Q*, *83*, 21. (2003)

[5]. Pagano, L., Russo, C., Sica, S., Costigliola, R. M.,. Limit states in earth dams during seismic and post-seismic stages. Theme Lecture in Proceedings of the VII ICEGE 7th International Conference on Earthquake Geotechnical Engineering. Rome 17-20 June 2019. Proceedings in Earth and geosciences. Francesco Silvestri &Nicola Moraci (Eds.), Published by: CRC press / Balkema - www.crcpress.com, ISBN 978-0- 367-14328-2 – V.4 pp.600-616 Theme Lecture. (2019).

[6]. Seed, H. B., Lee, K. L., Idriss, I. M., & Makdisi, F. I. The slides in the San Fernando dams during the earthquake of February 9, 1971. *Journal of the Geotechnical Engineering Division*, *101*(7), 651-688. (1975). https://doi.org/10.1061/AJGEB6.0000178

[7]. Seed, H. B., Seed, R. B., Harder, L. F., & Jong, H. L. Re-Evaluation of the Lower San Fernando Dam. Report 2: Examination of the Post-Earthquake Slide of February 9, 1971. *Available from the National Technical Information Service, Springfield, VA. 22161 as AD-A 214722. Price codes: A 12 in paper copy*. (1989).

[8]. Charatpangoon, B., Kiyono, J., Furukawa, A., & Hansapinyo, C. Dynamic analysis of earth dam damaged by the 2011 Off the Pacific Coast of Tohoku Earthquake. *Soil Dynamics and Earthquake Engineering*, *64*, 50-62. (2014). https://doi.org/10.1016/j.soildyn.2014.05.002

[9]. Harder, L. F., Kelson, K. I., Kishida, T., & Kayen, R. Preliminary observations of the Fujinuma dam failure following the March 11, 2011 Tohoku Offshore Earthquake, Japan. *Geotechnical Extreme Events Reconnaissance Report No. GEER-25e*. (2011).

[10]. Masini, L., & Rampello, S. La risposta di grandi dighe di terra durante eventi sismici intensi.

[11]. Newmark, N. M. Effects of earthquakes on dams and embankments. *Geotechnique*, *15*(2), 139-160. (1965).

[12]. Makdisi, F. I., & Seed, H. B. Simplified procedure for estimating dam and embankment earthquake-induced deformations. *Journal of the Geotechnical Engineering Division*, *104*(7), 849-867. (1978).https://doi.org/10.1061/AJGEB6.0000668

[13]. Yegian, M. K., Marciano, E. A., & Ghahraman, V. G. Earthquake-induced permanent deformations: probabilistic approach. *Journal of Geotechnical Engineering*, *117*(1), 35-50. (1991).

https://doi.org/10.1061/(ASCE)0733-9410(1991)117:1(35)

[14]. Bilotta, E., Pagano, L., & Sica, S. Effect of ground-motion asynchronism on the equivalent acceleration of earth dams. *Soil Dynamics and Earthquake Engineering*, *30*(7), 561-579. (2010). https://doi.org/10.1016/j.soildyn.2010.01.014

[15]. Alonso, E. E., & Pinyol, N. M. Unsaturated soil mechanics in earth and rockfill dam engineering. In Unsaturated Soils. Advances in Geo-Engineering (pp. 19-48). CRC Press. (2008).

[16]. Alonso, E. E., & Cardoso, R. Behavior of materials for earth and rockfill dams: Perspective from unsaturated soil mechanics. *Frontiers of Architecture and Civil Engineering in China*, *4*, 1-39. (2010).

[17]. Ariyan, M., Habibagahi, G., & Nikooee, E. Seismic response of earth dams considering dynamic properties of unsaturated zone. In *E3S Web of Conferences* (Vol. 9, p. 08002). EDP Sciences. (2016). https://doi.org/10.1051/e3sconf/20160908002

[18]. Fredlund, D. G., & Krahn, J. (1977). Comparison of slope stability methods of analysis. Canadian geotechnical journal, 14(3), 429-439. (1977). https://doi.org/10.1139/t77-045

[19]. Richards, L. A. Capillary conduction of liquids through porous mediums. *physics*, *1*(5), 318-333. (1931)

[20]. Geostudio (2018) GeoSlope International. Manual.

[21]. Heitland, J., Williams, J., Wanninayake A., Seepage Models – Tips, Tools & Guidance (From an Engineer's Perspective). *Dam Safety, National Conference of the Association of State Dam Safety Officials*. (2020).